A RISK-BASED SECURITY INDEX FOR DETERMINING OPERATING LIMITS IN STABILITY-LIMITED ELECTRIC POWER SYSTEMS

James D. McCalley, Member A.A. Fouad, Fellow
Vijay Vittal, Sr. Member Agustín A. Irizarry-Rivera, St. Member
Iowa State University

Baj L. Agrawal, Fellow
Arizona Public Service Company

Richard G. Farmer, Fellow
Arizona State University

Abstract: This paper is motivated by a concern that dynamic security limits based on the most severe contingency and scenario often result in operating restrictions corresponding to low or no risk but very high costs. A new risk-based security index is presented which accounts for both probability and impact of instability and is useful in determining operating limits. The approach is illustrated for a stability-limited system in Arizona.

Keywords: Power systems, transmission, stability, dynamic security, probability, risk, operating limits.

1.0 INTRODUCTION

The goal of this paper is to present an assessment approach for stability-limited systems that enables explicit quantification of the risk associated with a given operating point and subsequent determination of a risk-based operating limit. This goal, suggested in [1] by the IEEE PES APM Working Group, is motivated by a perception that today's deterministic security assessment approach often results in costly operating restrictions that are not justified by the corresponding low level of risk. It is envisioned that the risk-based approach would be implemented initially in an operations planning environment to compute limits used in making real time operating decisions. In this paper, we are interested only in application of the approach to stability-limited systems; however, we believe the concept of operating limit assessment via quantification of risk is applicable to limits imposed by any type of security problem.

1.1 COMPARISON TO DETERMINISTIC APPROACH

The traditional security assessment approach for developing operating limits, referred to in this paper as the deterministic approach, typically adheres to the following steps:

1. Develop a base case model of the planned operating system for the period under consideration, and identify the critical parameters which are to be maximized. These critical parameters are typically generation levels for specific generators and power transfers over specific transmission paths.

2. Develop a contingency list for each critical parameter. Traditionally, this has been done based on experience and knowledge of one's system; however, analytical techniques are becoming available [2].

3. Identify the most limiting credible contingency, or contingencies, for each critical parameter. Applicable utility or regional council criteria generally defines what constitutes a limiting credible contingency.

4. Identify the limit for each critical parameter as the level where system performance following the most limiting contingency first violates minimum operating reliability criteria.

The criterion for judging operating point acceptability is then based on the identified limit. An operating point beyond this limit is unacceptable.

One IEEE Standard definition for risk is the "product of probability and consequence" [3]. This definition captures the essence of the index used for security evaluation in the risk-based approach proposed in this paper. This risk-based approach builds from the deterministic approach in that steps 1 and 2 are retained. However, the risk-based approach departs from the deterministic approach in the following fundamental way. Whereas the deterministic approach develops limits based on the most severe contingencies, the risk-based approach develops limits based on a composite measure computed from a risk contribution from all contingencies in the list, where risk is the product of probability and consequence. Therefore, in the risk-based approach, analysis is required for all contingencies in the list and not just the most severe. Although this requirement could result in additional labor, this is a reasonable price to pay to gain the benefits associated with a more quantitative assessment of the security versus economy tradeoff.

The main difference in the two approaches resides not in the methods used to obtain results regarding system performance following a specific contingency; indeed the same methods are required in both approaches. Instead, the main difference in the two approaches resides in the criterion used to judge operating point acceptability. Whereas one uses a deterministic criterion (stable or unstable for most severe contingency under worst-case disturbance scenario), the other uses a criterion based on probability and consequence (composite risk level from all contingencies). Therefore the risk-based approach does not necessarily replace the deterministic approach; *it extends it.* One of the appeals of this approach is ease of transition for system operators; the change is transparent to the operators except for new graphs and tables.

1.2 REVIEW OF PREVIOUS WORK

A review of previous work on probabilistic stability assessment indicates a considerable amount of literature is available; only a representative sample of the main approaches are referenced in what follows. Anderson, Bose, and colleagues [4, 5] propose computing a stability distribution from probabilistic representation of the event space: disturbance location, type, and sequence. They also employ Monte Carlo simulation in this computation [6].

96 SM 505-8 PWRS A paper recomemended and approved by the IEEE Power System Engineering Committee of the IEEE Power Engineering Society for presentation at the 1996 IEEE/PES Summer Meeting, July 28 - August 1,1996, in Denver, Colorado. Manuscript submitted January 2, 1996; made available for printing May 17, 1996.

0885-8950/97/$10.00 © 1996 IEEE

Authorized licensed use limited to: Wuhan University. Downloaded on February 10,2024 at 11:16:48 UTC from IEEE Xplore. Restrictions apply.

Billinton and Kuruganty [7, 8, 9] compute a probability distribution for critical clearing time based on reliability of fault clearing devices and probabilistic representation of location and fault type. Wu et al. [10], propose an approach based on a time to insecurity. Silverstein and Porter [11] provide a disturbance-performance table for planning where lower performance levels are acceptable for events that are less likely to occur. Alvarado et al. [12] use the idea of security regions to develop an expected outage cost for voltage instability. Leite da Silva et al., [13] develop a framework for integrating adequacy and security assessment, resulting in computation of probabilistic indices for predisturbance conditions. Counan, et al. [14] devise a defense plan against extremely low probability but very severe system collapse mechanisms. Porretta, et al. [15] develop a risk-based index that is appropriate for use in a planning environment. Dodu and Merlin [16] use Monte Carlo simulation to estimate expected energy not served due to transient instability. The IEEE PES APM Working Group [1] presents a broad assessment of trends and needs in reliability practices; one of the needs identified was a risk assessment index for power system operation.

2.0 QUANTIFICATION OF RISK

For the purposes of this paper, we designate two types of instability: $j = 1$ indicates transient instability, i.e., loss of synchronism during the first few swings due to lack of synchronizing torque, $j = 2$ indicates oscillatory instability, i.e., sustained or negatively damped oscillations due to lack of damping torque. We define the risk R_{jip} associated with instability j due to an event (contingency) i while operating at point p as the product of probability of instability P_{jip} and impact I_{jip}

$$R_{jip} = P_{jip} I_{jip} \tag{1}$$

Higher values of R_{jip} indicate higher values of risk. We describe the two factors comprising R_{jip} in Subsections 2.1 and 2.2. In Subsection 2.3, we discuss computation of composite risk.

2.1 PROBABILITY OF INSTABILITY

We desire to choose limits in terms of risk associated with defined events known to potentially cause specific instabilities. The limits, characterized in terms of operating parameters, are associated with a given topological state of the system; when the state changes, new limits are used. We therefore assume that the topological state just previous to occurrence of the event is known with probability equal to one. Additionally, in keeping with traditional security assessment practices, we assume noncredible events[1] have probability zero. Therefore, in determining limits for the event "outage of circuit i," the probability of all other circuits *not failing* is one. The implication of these two assumptions is that in computing the probability of instability associated with an event, we will consider only the probability of the state transition from the present state to the state brought about by the event, which is the probability of occurrence of the event.

[1] Normally, credible events include those resulting in loss of a single component (so-called "N-1" events), and noncredible events include those resulting in simultaneous loss of more than one component. This general criteria could be more explicitly defined using a threshold on probability.

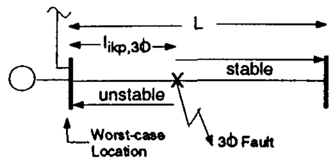

Figure 1: Illustration of Maximum Distance Function $l_{jip,3\phi}$

Let K_{jip} denote the event instability j due to event i at operating point p and $P(K_{jip})$ denote the probability of occurrence of this event over a specified time period. Let E_i denote the event line outage on transmission circuit i over a time period and $P(E_i)$ denote the probability of this event. The probability of instability j due to event i at operating point p is the product of the probability of event i and the conditional probability of instability j given event i occurs, i.e,

$$P(K_{jip}) = P(E_i)P(K_{jip}/E_i) \tag{2}$$

We make a critical departure from deterministic security assessment in that $P(K_{jip})$ allows that faults may be located anywhere on a circuit and not just at the most severe location, and that it may be three phase, two phase to ground, or single phase to ground, and not just three phase.

<u>*Conditional Probability of Instability:*</u> We assume that a fault may occur anywhere on a line with the same probability of occurrence. The uniform probability distribution function is used to obtain the probability of instability j given that event i (outage of circuit i) is caused by an n phase ($n\phi$) fault on circuit i. This probability is given by

$$P(K_{jip}/n\phi fault) = \int_{l_{jip,n\phi}} \frac{1}{L_i}\,dx = \frac{l_{jip,n\phi}}{L_i} \tag{3}$$

The parameter $l_{jip,n\phi}$ indicates the maximum distance from the worst-case location for which an $n\phi$ fault results in unstable response, or equivalently, the minimum distance from the worst-case location for an $n\phi$ fault results in stable response. For a transient instability problem, the worst-case location is normally the bus closest to the machine at risk for losing synchronism. This maximum distance function is illustrated in Figure 1 for a 3ϕ fault.

If the generation level is at or below its deterministic limit (e.g., the maximum generation level for which the generator response is stable for a three phase fault at the machine terminals), then $l_{jip,3\phi} = 0$, implying that the generator response is stable for a three phase fault located anywhere on the line. In this case, we would expect $l_{jip,2\phi} = l_{jip,1\phi} = 0$, also. At some generation level above the deterministic limit, however, it would be true that $l_{jip,3\phi} \geq x$, implying that the generator response is unstable for a three phase fault located within a distance of x from the generator terminals. At the generation level where $l_{jip,3\phi} = x$, it would be likely that $0 \leq l_{jip,1\phi} \leq l_{jip,2\phi} < x$, i.e., single phase to ground and double phase to ground faults would be stable for faults closer to the generator terminals than x.

Authorized licensed use limited to: Wuhan University. Downloaded on February 10,2024 at 11:16:48 UTC from IEEE Xplore. Restrictions apply.

The previous discussion indicates the reason for subscript p in $l_{jip,3\phi}$, $l_{jip,2\phi}$, and $l_{jip,1\phi}$; these variables are dependent on the operating point p, where the operating point is characterized by the critical parameter. In the case of transient instability, one of the critical parameters is usually the generation level of the plant at risk for going out of step. Analytic expressions for the dependency of l_{jip} on the critical parameter are generally not apparent for multimachine systems. However, it is possible to obtain data characterizing this dependency by using time domain simulation or other techniques to find the limiting values of the critical parameter for various fault locations on the line[2]. This data can then be fit with appropriate functions to obtain $l_{jip,3\phi}$, $l_{jip,2\phi}$, and $l_{jip,1\phi}$ as a function of the critical parameter.

We define 3ϕ, 2ϕ, and 1ϕ faults to be the set of all possible faults,[3] and we assume that only one of these faults occur at a time. This constitutes a collection of mutually exclusive and exhaustive events. We may use the Law of Total Probability to obtain the desired probability of instability j due to event i at p.

$$\begin{aligned} P(K_{jip}) &= \sum_{n=1}^{3} P(n\phi fault)P(K_{jip}/n\phi fault) \\ &= \sum_{n=1}^{3} P(n\phi fault)\frac{l_{jip,n\phi}}{L_i} \end{aligned} \tag{4}$$

Assume we know the probability of the event occurrence of a $n\phi$ fault given a fault occurs on line i at operating point p over a specified time period, i.e., $P(n\phi fault/E_i)$, where $P(n\phi fault/E_i)$ is denoted by $f_{n\phi}$. Since the probability of having a fault on line i given an $n\phi$ fault occurred, $P(E_i/n\phi fault)$, is equal to one, we have from the definition of conditional probability,

$$P(n\phi fault) = P(E_i)P(n\phi fault/E_i) = P(E_i)f_{n\phi} \tag{5}$$

Substitute Eq. 5 into Eq. 4 to obtain

$$P(K_{jip}) = P(E_i)\sum_{n=1}^{3} f_{n\phi}\frac{l_{jip,n\phi}}{L_i} \tag{6}$$

Probability of Occurrence of Event i, $P(E_i)$: In contrast to making real-time risk calculations for each operating point, we are computing risk off-line to compare the severity of different candidate limits in a way that reflects the probability and impact of instability. Using risk in this comparitive fashion provides that the choice of time period for which $P(E_i)$ is computed is not critical; we choose a time period of one year.

Having chosen one year as the time period, we may use a homogeneous Poisson process (HPP) [17, pp. 105] to model transmission circuit outages with the process intensity (rate of occurrence) estimated as the observed number of outages divided by the number of observation intervals. The HPP is given by

$$P(E_i) = \lambda_i e^{-\lambda_i}, \lambda_i > 0 \tag{7}$$

where $P(E_i)$ is the probability of event i occuring in the next year, and λ_i is the intensity. To account for the non-uniformity of outage rates we use different intensities depending on season and weather, e.g., summer normal, winter storm.

2.2 IMPACT OF INSTABILITY

We denote the impact of instability j due to event i as I_{jip}. In general, there are two main components; impact of unsupplied energy and social/political impact.

Unsupplied Energy: B_{jip}, in per unit energy, represents the impact associated with the increase in production costs caused by replacing the lost energy supply with more expensive energy. It is given by

$$B_{jip} = \frac{P_{lost_{jip}} T_{lost_{ji}}}{P_{peak}(1hour)} \tag{8}$$

where $P_{lost_{jip}}$ is the generating level of the units lost, P_{peak} is the peak load for the system, and $T_{lost_{ji}}$ is the time required to resynchronize and load the lost units. The per unit base is the energy supplied to the entire system for 1 hour under peak conditions.

Social/Political Impact: C_{ji} represents the impact associated with social and political factors such as regulatory and customer reponse. This factor gives the percentage increase over the energy replacement impact. The impact of regulatory response on the utility could be considerable if the lost plant is a nuclear unit. The impact of customer response on the utility could be considerable if service is interrupted. C_{ji} may be computed using

$$C_{ji} = \sum_{s \in i} C_{jis} \tag{9}$$

where C_{jis} are impact factors giving the percentage increase over the energy replacement impact for a specific impact s. Table 1 gives a sample of preliminary estimates for various impact factors. Equation 9 provides for the case when an event results in several impacts. For example, if event i causes tripping all n units at a fossil fired plant, resulting in a black plant condition, then

$$C_{ji} = n(C_{ji2}) + C_{ji3} = n(0.1) + 1.0$$

Table 1: Impact Factors

Description of Impact	Numerical Designation s	C_{jis}
Trip gas turbine	1	0.01
Trip of fossil-fired unit	2	0.10
Black plant	3	1.00
Trip of a nuclear unit	4	2.00
System separation (islanding)	5	3.00
System Blackout	6	100.

[2]The effects of single and double line to ground faults on the positive sequence network may be approximately captured by modeling an effective fault impedance of $X_e = X_0 + X_2$ for a single line to ground fault and $X_e = \frac{X_0 X_2}{X_0+X_2}$ for a double line to ground fault, where X_0 and X_2 are the zero sequence and the negative sequence reactances, respectively, between the fault point and the neutral.

[3]Line to line faults may also be included if desired.

Authorized licensed use limited to: Wuhan University. Downloaded on February 10,2024 at 11:16:48 UTC from IEEE Xplore. Restrictions apply.

The total impact of instability j resulting from contingency i at operating point p is the energy impact increased by the percentage $100(C_{ji})\%$, i.e.,

$$I_{jip} = B_{jip}(1 + C_{ji}) \tag{10}$$

The $(1+C_{ji})$ social/political weighting is based on subjective assessment and is approximate. There may be better methods of including this effect; nonetheless, the point to be made here is that it represents real impacts having effects that must be included in the risk index.

2.3 COMPOSITE RISK

Risk may be interpeted as an *expectation* [18, p. 215 - 222] of the impact over the unit of time for which probability is measured. A composite risk may be obtained as the summation over risks of each individual event [19, p.301]. Summing individual risks is appropriate if all impacts are computed in the same units.

The composite risk at an operating point p associated with a particular instability j is the sum of the risks from all M events having potential to cause the instability:

$$R_{jp} = \sum_{i=1}^{M} R_{jip} \tag{11}$$

Likewise, the composite risk at an operating point p associated with several different instabilities is given by

$$R_p = \sum_{j=1}^{N} R_{jp} = \sum_{j=1}^{N}\sum_{i=1}^{M} R_{jip} \tag{12}$$

where there are N different instabilities that have potential to occur.

3.0 EXAMPLE

A 1443 bus, 126 generator reduced equivalent model of the WSCC system, representing summer peak conditions, is used to illustrate the risk-based approach. The study area consists of the 500 kV system local to the Navajo Power Plant in Arizona. The system configuration, illustrated in Figure 2, represents the Navajo-McCullough 500 kV line out of service due to either forced or scheduled outage. It is assumed that there is no series compensation in the Navajo-Westwing, Navajo-Moenkopi, Moenkopi-Westwing, and Moenkopi-Eldorado 500 kV lines. Generators in the study area are represented using a two axis model with exciter, power system stabilizer, and turbine-governor representation. Real power loads are represented as constant current, and reactive power loads are represented as constant impedance. To clearly and simply illustrate the basic concepts of risk-based security assessment, this example does not include the effects of remedial actions that would normally be used under these conditions.

It is desired to identify operating regions in terms of two parameters: P_{NAV}, the generation level at the Navajo plant, and P_{WF}, the transfer for the Western flow[4]. There are two events known to constrain the Navajo generation

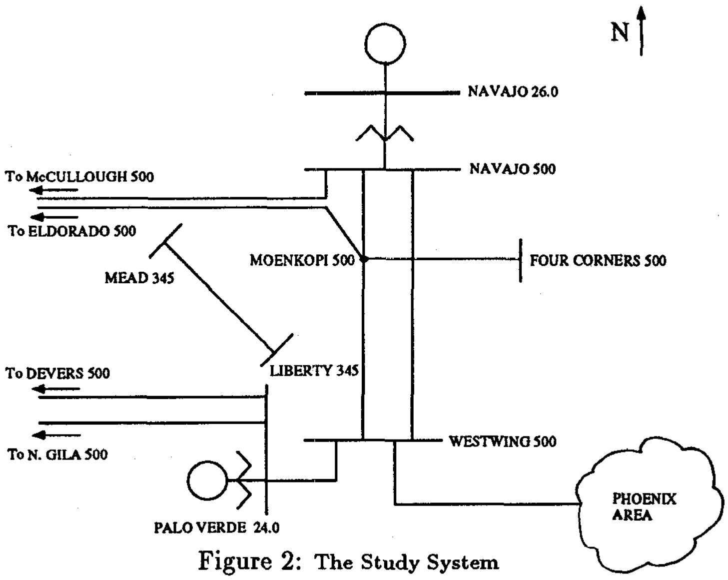

Figure 2: The Study System

below its 2250 MW rating due to transient instability. These are (1) Loss of the Navajo-Moenkopi 500 kV line, and (2) Loss of the Navajo-Westwing 500 kV line. There is one event known to constrain the Western flow due to oscillatory instability. This is (3) Loss of the Palo Verde-North Gila 500 kV line.

3.1 FAULT RATE OF OCCURRENCE & TYPE

Historical data indicates that faults occur at an average rate of 0.4 per year per 100 miles of transmission. We assume that this rate applies during summer normal weather conditions. Table 2 computes the Poisson process intensity λ_i based on this factor.

Table 2: Intensity (Rate of Occurrence) for Three Events

Event No. (i)	Transmission Line Faulted	Length (miles)	λ_i $\frac{events}{year}$
1	Navajo-Moenkopi	76	0.304
2	Navajo-Westwing	259	1.036
3	Palo Verde-N. Gila	116	0.464

No historical data was available regarding the type of fault, so the following percentages were assumed for all events: $f_{3\phi} = 0.01$, $f_{2\phi} = 0.19$, and $f_{1\phi} = 0.8$.

3.2 DETERMINISTIC LIMITS

The deterministic limits are based on the worst-case disturbance scenario for each event. For events 1 and 2, this scenario consists of a three phase, four cycle fault at the Navajo 500 kV bus. For event 3, this scenario consists of a three phase, four cycle fault at the Palo Verde 500 kV bus. The deterministic stability limits for each event were identified using time domain simulation and are given in Table 3.

Table 3: Deterministic Limits

Event No. (i)	Critical Parameter	Limit (MW)
1	Navajo generation, P_{NAV}	1325
2	Navajo generation, P_{NAV}	1995
3	Western flow, P_{WF}	4030

[4] The Western flow is the sum of flows on the Liberty-Mead 345 kV line and the following 500 kV lines: Navajo-McCullough, Moenkopi-Eldorado, Palo Verde-Devers, and Palo Verde-North Gila.

Authorized licensed use limited to: Wuhan University. Downloaded on February 10,2024 at 11:16:48 UTC from IEEE Xplore. Restrictions apply.

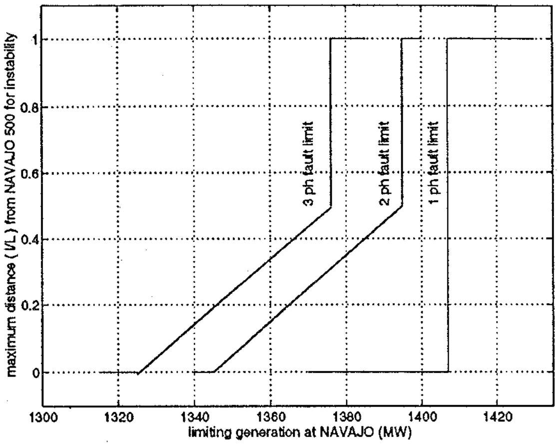

Figure 3: Normalized maximum fault location distances for instability for event 1

3.3 MAXIMUM DISTANCE FUNCTIONS

The maximum distance functions, $l_{jip,n\phi}$, were determined for the three events $i = 1$ (Navajo-Moenkopi), $i = 2$ (Navajo-Westwing), and $i = 3$ (Palo Verde-North Gila) using time domain simulation to identify limits for faults located at various locations on the line to be cleared. These functions, for event 1, normalized by dividing by line length, are illustrated in Figure 3; those for events 2 and 3 are numerically different but similar in form and are therefore not illustrated.

All functions are equal to 0 when the critical parameter is less than a certain value; this means that all faults of the indicated type ($3\phi, 2\phi$, or 1ϕ) result in stable system performance for this range of critical parameter. Likewise, all functions are equal to 1 when the critical parameter is greater than a certain value; this means that all faults of the indicated type result in unstable system performance for the corresponding range of the critical parameter.

3.4 ENERGY IMPACT

The energy impact for all three events is caused by loss of generation. If either events 1 or 2 result in an out of step condition at the Navajo plant, requiring trips of all three units, it is estimated that the plant would be out of service for 10 hours. Assuming a system peak of 22,500 MW, the corresponding energy impact factors are

$$B_{11p} = B_{21p} = \frac{(P_{NAV})(10hours)}{(22,500MW)(1hour)}$$

If event 3 results in Arizona-California separation, it is estimated that 2250 MW of generation would trip and be out of service for 10 hours. Thus,

$$B_{32p} = \frac{(2250MW)(10hours)}{(22,500MW)(1hour)} = 1.0$$

3.5 SOCIAL/POLITICAL IMPACT

Since events $i = 1$ and $i = 2$ may result in transient instability requiring trips of three fossil-fired units giving a black plant condition, reference to Table 1 indicates that C_{ji} for both events is $C_{11}=C_{21}=3(C_{ji2})+C_{ji3}= 3(0.1)+1.0 = 1.3$. Event 3, resulting in Arizona-California separation, has $C_{32} = 3.0$.

3.6 CHARACTERISTICS OF RISK INDEX

Because the system performance for the three events are dependent on only two critical parameters, the deterministic security regions may be illustrated on a single two-dimensional diagram as in Figure 4. The horizontal line drawn at 1325 MW indicates the maximum Navajo generation for which event 1 is secure; the horizontal line drawn at 1995 MW indicates the maximum Navajo generation for which event 2 is secure; the vertical line drawn at 4030 MW indicates the maximum Western Flow for which event 3 is secure. Risk computations for operating points 1-11, illustrated on Figure 4, are summarized in Table 4. These data illustrate several interesting characteristics of the proposed risk index.

Effect of Maximum Distance Functions $l_{jip,3\phi}$, $l_{jip,2\phi}$, $l_{jip,1\phi}$: The variation in risk contribution from event 1 due to limiting operating point functions can be observed in the risk computations for points 1-4 in Table 4, where risk increases from 0 to 0.3267. Operating point 1 (P_{NAV}=1325 MW, R_p=0) incurs no risk because it is stable for all fault types, as shown in Figure 3 where $l/L = 0$ for all fault types. Operating point 2 (P_{NAV}=1385 MW, R_p=0.0273) incurs all risk for 3ϕ faults and partial risk for 2ϕ faults, operating point 3 (P_{NAV}=1405 MW, R_p=0.0644) incurs all risk for 3ϕ and 2ϕ faults, and operating point 4 (P_{NAV}=1425 MW, R_p=0.3267) incurs all risk for all fault types. Similar analysis applies for risk contributions from event 2 (operating points 5-8) and event 3 (operating points 8-11).

Effect of Fault Type Distributions $f_{3\phi}, f_{2\phi}, f_{1\phi}$: The large increase in risk between operating points 3 and 4 is caused by the influence of 1ϕ faults. Operating point 3 incurs no risk for 1ϕ faults, whereas operating point 4 incurs all risk

Table 4: Summary of Risk Computations for 11 Operating Points

p Op. Pt.	Navajo Gen P_{NAV} (MW)	Western Flow P_{WF} (MW)	Event 1 Risk i=1,k=1 R_{ikp}=R_{11p}	Event 2 Risk i=2,k=1 R_{ikp}=R_{21p}	Event 3 Risk i=3,k=2 R_{ikp}=R_{32p}	Composite Risk Events 1, 2, & 3 R_p= R_{11p}+R_{21p}+R_{32p}
1	1325	4030	0.0000	0.0000	0.0000	0.0000
2	1385	4030	0.0273	0.0000	0.0000	0.0273
3	1405	4030	0.0644	0.0000	0.0000	0.0644
4	1425	4030	0.3267	0.0000	0.0000	0.3267
5	1995	4030	0.4575	0.0000	0.0000	0.4575
6	2165	4030	0.4964	0.0215	0.0000	0.5179
7	2215	4030	0.5079	0.1665	0.0000	0.6744
8	2250	4030	0.5159	0.8456	0.0000	1.3615
9	2250	4060	0.5159	0.8456	0.0257	1.3872
10	2250	4115	0.5159	0.8456	0.5741	1.9356
11	2250	4170	0.5159	0.8456	1.1670	2.5285

Authorized licensed use limited to: Wuhan University. Downloaded on February 10,2024 at 11:16:48 UTC from IEEE Xplore. Restrictions apply.

for 1ϕ faults. The influence of 1ϕ faults is greater than that of 2ϕ and 3ϕ faults because fault type probability (see Section 2.1) $f_{1\phi} = 0.8$ as compared to $f_{3\phi} = 0.01$ and $f_{2\phi} = 0.19$, i.e., 80% of all faults are 1ϕ. This effect may also be observed for event 2 by comparing operating points 7 and 8. This effect is not as pronounced for event 3 because oscillatory instability is less sensitive to fault type.

Effect of intensity λ: Comparison between the risk contribution from event 1 to the risk contribution from event 2 for operating point 8 indicates that the event 2 risk (0.8456) is substantially larger than the event 1 risk (0.5159). This effect is entirely attributed to the differences in λ_i for the two events: $\lambda_1 = 0.304$ and $\lambda_2 = 1.036$.

Effect of Energy Impact B_{jip}: Inspection of event 1 risk in Table 4 for operating points 5-8 indicates that this component of risk increases from 0.4575 to 0.5159. This increase in risk is entirely attributed to the increase in B_{11p} caused by increased generation level at Navajo from 1995 MW to 2250 MW.

Effect of Social/Political Impact C_{ji}: Comparison of the risk contributions from events 1 and 3 for operating point 11 in Table 4 indicates that event 3 risk (1.1670) is substantially larger than event 1 risk (0.5159). Because the energy impacts are the same for both events (2250 MW), the intensities are similar ($\lambda_1 = 0.304$ and $\lambda_3 = 0.464$), and this operating point is unstable for all faults for both events, almost all of this difference is attributed to the influence of social/political impact weighting; $C_{11} = 1.3 \Rightarrow (1+C_{11}) = 2.3$, and $C_{32} = 3.0 \Rightarrow (1 + C_{32}) = 4.0$.

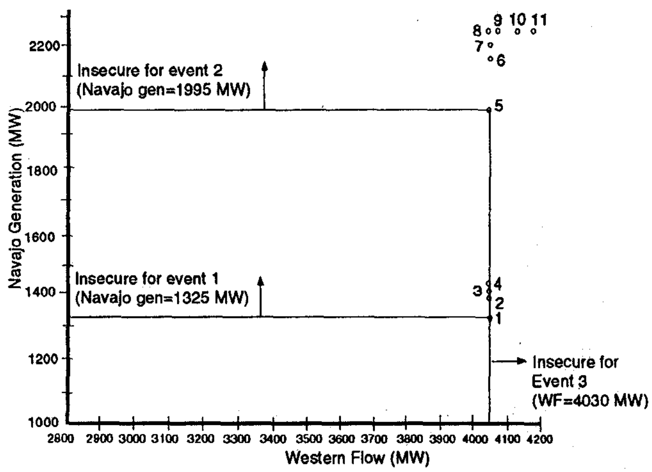

Figure 4: Deterministic Security Regions for the Three Events

3.7 CONTOURS OF CONSTANT RISK

Variation of risk with operating points can be most clearly illustrated by drawing contours of constant risk in the space of critical parameters. This is shown in Figure 5 for our example. These contours would be very useful in an operating environment; some particularly interesting features are as follows.

- Operation within the deterministic limits corresponding to $P_{NAV} = 1325$ MW and $P_{WF} = 4030$ MW incurs zero risk.
- For $P_{WF} \leq 4030$ MW, as P_{NAV} increases from 1325 MW to 1405 MW, risk increases gradually to 0.06 due to the influence of 3ϕ and 2ϕ to ground faults; therefore an additional 80 MW of output can be obtained with very little increase in risk. However, the risk jumps dramatically from 0.06 to 0.32 as P_{NAV} increases from 1405 MW to about 1425 MW. As previously mentioned, this jump is due to the influence of 1ϕ faults. The 1425 MW operating point is therefore not attractive under most circumstances, since only a 20 MW curtailment substantially reduces the risk. A similar situation occurs for higher Navajo generation levels. As P_{NAV} increases from 2245 MW to 2250 MW, the risk jumps from 0.85 to 1.36. The 2250 MW operating point is therefore not attractive under most circumstances, since only a 5 MW curtailment substantially reduces the risk.
- The least restrictive (most risky) contour drawn for $P_{NAV} = 2250$ MW, where the risk is 1.36, does not extend to the Western flow axis because it is not possible to incur this high risk level by increasing P_{WF} for lower values of P_{NAV} since the maximum risk contribution from event 3 is 1.167 (see Table 4).
- The contours are closely spaced for low P_{NAV} and high P_{WF} because the oscillatory instability problem caused by event 3 is not very sensitive to fault type or location.

The contours in Figure 5 are drawn for a specific fault type distribution assumed for this example. A different fault type distribution could be used if appropriate.

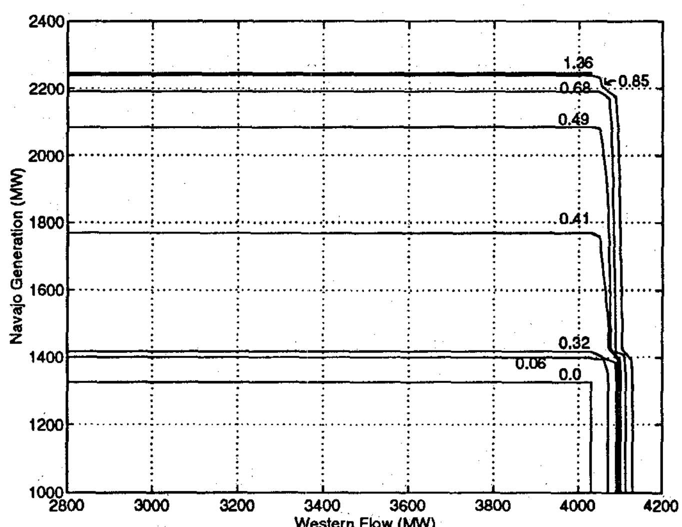

Figure 5: Contours of Constant Risk

4.0 DEVELOPMENT OF OPERATING LIMITS

A key step in using the proposed security assessment approach is development of risk-based operating limits. It is desirable to develop these limits so that the system operator still sees the same tabular and graphical form as under

Authorized licensed use limited to: Wuhan University. Downloaded on February 10,2024 at 11:16:48 UTC from IEEE Xplore. Restrictions apply.

the deterministic approach. Determination of a threshold risk value would provide for identification of the desired limits by calculation of the appropriate constant risk contour.

Reference [1] suggests three different methods of identifying thresholds for a new index, as follows.

1. Use judgement or experience based on what has previously been defined as acceptable operating points in the past.

2. Compute a criterion for the index in terms of other indices for which criteria are clearly established.

3. Perform a cost/benefit analysis, and choose a criterion that minimizes total costs of providing reliability plus the costs of instability.

We believe that method 1 should be applied initially in order to gain experience with the risk index and to provide a link to the deterministic approach so that the transition from one approach to another is more acceptable to system operators. This method could be applied by computing risk for acceptable operating points where system response to a contingency is stabilized by applying remedial action to trip a unit.

Method 2 is attractive if other criteria for stability limitations can be established. For example, one might propose that loss of one Navajo unit (750 MW) for 10 hours once per year is acceptable, but loss of one unit for 10 hours twice per year is unacceptable, so that the expected impact is bracketed between $[(750)(10)/22,500](1+0.1) = 0.367$ and $2\times 0.367 = 0.733$. Acceptance of 0.367 as the risk threshold would result in an operating region expansion from the deterministic limit of 1325 MW Navajo generation to about 1600 MW.

Threshold determination by method 3 could be interpreted as an optimization problem where one desires to simultaneously minimize the sum of the operating costs plus the risk. The index developed in this paper provides a means of formulating this problem for stability-limited systems. Application of these three methods to identify a threshold level of acceptable risk is the subject of our ongoing work.

5.0 CONCLUSIONS

We have proposed a new approach for performing security assessment for stability-limited electric power systems. This approach retains the basic tools and procedures of the traditional deterministic approach, but it also extends it in computing risk, which accounts for probability and impact of instability. Application of the risk-based approach was illustrated for a transient instability problem and an oscillatory instability problem occuring in a test model of the WSCC system. Two important attributes which distinguish the risk-based approach from the deterministic approach are that the risk index is influenced by all defined contingencies and not just the most limiting one, and it accounts for variation in fault types and location instead of assuming a worst-case disturbance scenario. A first step in developing risk-based operating limits is to identify constant risk contours in terms of the parameters used to monitor security levels; we intend to experiment with several methods of identifying a specific risk-based limit in future work, where the goal will be to establish a basis for a general security assessment framework whereby the economic benefit of an operating point may be balanced against its risk to achieve an optimal operating strategy. We believe such a framework is particularly appropriate in the competitive environment towards which the electric power industry is moving.

References

[1] IEEE PES Task Force on Applications of Probability Methods, "Bulk Power System Reliability Criteria and Indices: Trends and Future Needs," *IEEE Trans. on Pwr. Sys.*, Vol. 9, No. 1, February 1994, pp. 181-190.

[2] EPRI Final Report TR-104352, Project RP 3103-3, "Analytical Methods for Contingency Selection and Ranking for Dynamic Security Analysis," September 1994.

[3] "The New IEEE Standard Dictionary of Electrical and Electronic Terms, 5th Edition," 1993, IEEE.

[4] P. Anderson and A. Bose, "A Probabilistic Approach to Power System Stability Analysis," *IEEE Trans. on Pwr. App. and Sys.*, Vol. PAS-102, No. 8, August 1983, pp. 2430-2439.

[5] P. Anderson, A. Bose, K. Timko, and F. Villaseca, "A Probabilistic Approach to Stability Analysis," EPRI Report EL-2797, 1983.

[6] K. Timko, A. Bose, and P. Anderson, "Monte Carlo Simulation of Power System Stability," *Proc. of the Power Industry Computer Applications Conference (PICA)*, 1983.

[7] R. Billinton and P. Kuruganty, "A Probabilistic Index for Transient Stability," *IEEE Trans. on Pwr. App. and Sys.*, Vol PAS-99, No. 1, Jan/Feb 1980.

[8] P. Kuruganty and R. Billinton,"A Probabilistic Assessment of Transient Stability," *International Journal of Electric Power and Energy Systems*, Vol 2, No. 2, April 1980.

[9] R. Billinton and P. Kuruganty, "Probabilistic Evaluation of Stability in Multimachine Power Systems," *IEE Proc.* Pt. C, Vol 126, No. 4, pp 321-326, 1980.

[10] F. Wu, Y. Tsai, and Y. Yu, "Probabilistic Steady-State and Dynamic Security Assessment," *IEEE Trans. Pwr. Sys.*," Vol. 3, No. 1, Feb. 1988, pp. 1-9.

[11] B. Silverstein and D. Porter, "Contingency Ranking for Bulk System Reliability Criteria," *IEEE Trans. Pwr. Sys.*," Vol. 7, Aug. 1992, pp 956-964.

[12] F. Alvarado, Y. Hu, D. Ray, R. Stevenson, and E. Cashman, "Engineering Foundations for the Determination of Security Costs," *IEEE Trans. Pwr. Sys.*," Vol. 6, Aug. 1991, pp. 1175-1182.

[13] A. Leite da Silva, J. Endrenyi, and L. Wang, "Integrated Treatment of Adequacy and Security in Bulk Power System Reliability Evaluations," *IEEE Trans. on Pwr. Sys.*, Vol. 8, Feb. 1993, pp 275-282.

[14] C. Counan, M. Trotignon, E. Corradi, M. Stubbe, and J. Deuse, "Major Incidents on the French Electric System: Potentiality and Curative Measures Studies," *IEEE Trans. on Pwr. Sys.*, Vol. 8, Aug. 1993, pp 879-886.

[15] B. Porretta, D. Kiguei, G. Hamoud, E. Neudorf, "A Comprehensive Approach for Adeqeuacy and Security Evaluation of Bulk Power Systems," *IEEE Trans. Pwr. Sys.*, Vol. 6, No. 2, May 1991.

[16] J. Dodu and A. Merlin, "New Probabilistic Approach Taking into Account Reliability and Operation Security in EHV Power System Planning at EDF," *IEEE Trans. on Pwr. Sys.*, Vol. PWRS-1, No. 3, Aug., 1986.

[17] L.J. Bain and M. Engelhardt, "Introduction to Probability and Mathematical Statistics", second edition PWS-KENT Publishing Company, 1992.

[18] G. Anders, "Probabilistic Concepts in Electric Power Systems," 1990, John Wiley & Sons, New York.

Authorized licensed use limited to: Wuhan University. Downloaded on February 10,2024 at 11:16:48 UTC from IEEE Xplore. Restrictions apply.

[19] M. Modarres, "Reliability and Risk Analysis," Marcel Dekker, Inc., New York, 1993.

Acknowledgement: We express our appreciation to Dr. H.T. David of the Iowa State University Department of Statistics for helpful discussion during the preparation of this paper.

Biographies

Baj L. Agrawal received his B.S. in Electrical Engineering from Birla Institute of Technology and Science, India, in 1970 and his M.S. and Ph.D. in Control Systems from the University of Arizona, Tucson, in 1972 and 1974, respectively. He joined the Arizona Public Service Company in 1974 and is now a Principal Engineer. His responsibilities include dynamic modeling and simulation of power system interaction with turbine generators, including the areas of power system stabilizer application, power system stability, subsynchronous resonance, and electric system transients. Dr. Agrawal is active in IEEE working groups related to dynamic performance and in industry committees of the Western Systems Coordinating Council. He has authored a number of papers on power system dynamic performance. He is a Fellow of the IEEE.

Richard G. Farmer received his B.S. in Electrical Engineering from Colorado State University in 1952 and his M.S. in Electrical Engineering from Arizona State University in 1964. He spent two years at the Massachusetts Institute of Technology Digital Computer Laboratory in Cambridge, Massachusetts. In 1955, he joined the firm of Miner and Miner Consulting Engineers, Inc., in Creely, Colorado, and was promoted to Vice President in 1961. In 1965, he was employed by Arizona Public Service Company in Phoenix, Arizona, where he spent 10 years in the System Planning Department followed by 19 years in charge of the Technical Projects Department. He was a Principal Engineer at the time of his retirement in 1994. From 1966 to 1994, Mr. Farmer was an Adjunct Professor at Arizona State University in Tempe, Arizona. He is presently a Faculty Research Associate at this institution. Mr. Farmer has authored many papers on power system stability and subsynchronous resonance. He served as Chairman of the IEEE System Dynamic Performance Subcommittee and the IEEE Subsynchronous Resonance Working Group. He is a Fellow of the IEEE.

A.A. Fouad is Professor of the Electrical and Computer Engineering Department at Iowa State University. He received the B.S. in Electrical Engineering (1950) at the University of Cairo; M.S. (1953) from the University of Iowa; and the Ph.D. (1956) from Iowa State University. He is the 1990 Anson Marston Distinguished Professor of Engineering at Iowa State University, and he is a Fellow of the IEEE.

A.A. Irizarry-Rivera received his B.S. in Electrical Engineering (1988) from the University of Puerto Rico at Mayaguez and his M.S. (1990) in Electrical Engineering from the University of Michigan at Ann Arbor. He is currently working toward a Ph.D. in power systems at Iowa State University. His interests include power system dynamics, probabilistic methods, and power system security assessment. Mr. Irizarry-Rivera is a registered professional engineer in Puerto Rico and an IEEE student member.

James D. McCalley is Assistant Professor of Electrical and Computer Engineering Department at Iowa State University, where he has been employed since 1992. He worked for Pacific Gas and Electric Company from 1986 to 1990. Dr. McCalley received the B.S. (1982), M.S. (1986), and Ph.D. (1992) degrees in Electrical Engineering from Georgia Tech. He is a registered professional engineer in California and a member of the IEEE.

Vijay Vittal is Professor of the Electrical and Computer Engineering Department at Iowa State University. He received the B.E. (1977) in Electrical Engineering from Bangalore, India, the M. Tech. (1979) from the Indian Institute of Technology, Kanpur, India, and the Ph.D. (1982) from Iowa State Univeristy, Ames, Iowa. He is the recipient of the 1983 Presidential Young Investigator Award. He is a senior member of the IEEE.

Authorized licensed use limited to: Wuhan University. Downloaded on February 10,2024 at 11:16:48 UTC from IEEE Xplore. Restrictions apply.

Discussion

R. BILLINTON, S. ABORESHAID AND M. FOTUHI-FIRUZABAD (Power Systems Research Group, University of Saskatchewan) The authors have presented a welcome contribution to the area of stochastic transient stability evaluation by extended the risk indices to consider the impact of instability. We have a number of comments and also some questions on which the authors' views would be appreciated.

1. The operational behavior of the protection system is an important factor which affects the security and service continuity associated with bulk power systems. Reference D1 shows that for a distance impedance scheme, the operating times can be adequately represented by normal distributions. Consequently, an approach to model the stochastic behavior of protection system components in probabilistic transient stability studies was presented in [D2, D3]. The question is: Why did the authors chose to use crisp values when modeling the protection system?.

2. In addition to the stochastic considerations presented in [D2, D3, 7-9], the authors have included the probability that an event i occurs during the studied period, $P(E_i)$. After choosing one year as the time period, the authors have modeled the transmission line outages by a homogeneous Poission process. Equation (7) presents a special case of the Poission probability distribution in which only the probability of one failure can happen in the time period of interest (one year). A more comprehensive representation for the probability of event occurrence is given by the following equation (one year period):

$$P_x(E_i) = \frac{\lambda_i^x \, e^{-\lambda_i}}{x!}$$

where $P_x(E_i)$ is the probability of an outage occurring x times in the studied period. A simple representation of the event probability of occurrence is presented in [D4]. The following figure shows both the occurrence density function and the cumulative distribution function of $P_x(E_2)$ for the case of a fault in the Navajo-Westwing. The authors have considered the case in which only one failure occurs in the line. The probability of having at least one fault in the line is 0.645. The authors have considered only 57% of this probability in their calculations. The remaining 43% which forms the probability of having more than one failure during the studied year was not taken into consideration. The authors comments regarding this matter is appreciated.

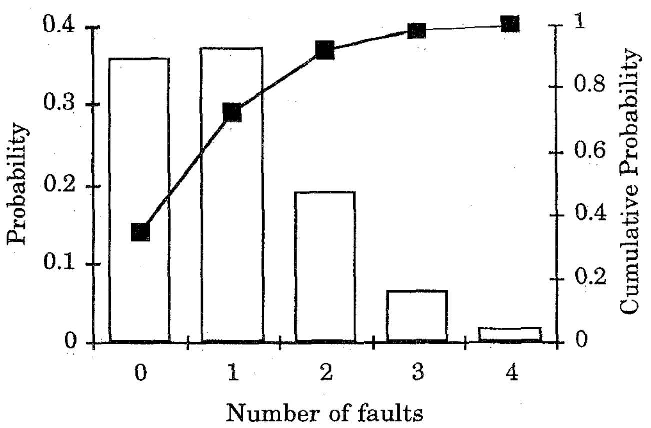

3. The authors state in page 3: "To account for the non-uniformity of outage rates we use different intensities depending on season and weather, e.g. summer normal, winter storm". In the studied system, the author chose a one year period to examine the system. However, by examining the results presented in Table 4, it appears that only the summer normal failure rates were considered in the analysis. The one year period will obviously have to be segmented into shorter periods during which the different occurrence rates apply.

4. In reading Section 3 of the paper, we found some difficulties in following the subscripts of the risk (R_{jip}), impact of unsupplied energy (B_{jip}) and social/political impact (C_{ji}). This is due to a typographical mistake in which the event number (i) and the instability type (j) are interchanged. Moreover k in Table 4 should be replaced by j. We are simply pointing out these errors to aid in reading this interesting paper.

References

D1. DeHass, J., "Determination of Time Settings in a Distance Protection Scheme Based on Statistical Methods", CIGRE Conference Proceedings, Vol. II, Paper 31-05, 1968.

D2. Kuruganty, P.R.S. and Billinton, R., "Protection System Modeling in a Probabilistic Assessment of Transient Stability", IEEE Transactions on Power Apparatus and Systems, Vol. PAS-100, pp. 2163-2170, 1981.

D3. Billinton, R., Aboreshaid, S. and Fotuhi-Firuzabad, M., "Probabilistic Transient Stability Studies Using the Method of Bisection", Paper # 96 WM 266-7 PWRS, Presented at the IEEE/PES Winter Power meeting, Jan. 21-25, 1996, Baltimore, MD. USA.

D4. Anders, G., *Probability Concepts in Electric Power Systems*, John Wiley & Sons, Inc., New York, 1990.

Manuscript received August 16, 1996.

J. McCalley, A. Fouad, V. Vittal, A. Irizarry-Rivera, B. Agrawal, and R. Farmer: We express our appreciation towards the discussers for their interest in our paper. Their comments are constructive and useful in clarifying important issues related to risk-based security assessment.

We emphasize that the intent of this paper is to motivate the need for extending the current practice of determining *operating limits* so that the decision is based on explicit quantification of event probability and event impact. We therefore associate a specific risk value for each operating condition. This is in contrast to the planning problem where specific risk values would be associated with different facility alternatives implemented over an extended time interval, and the calculation would entail summation over varying operating conditions.

Regarding the discussers' question in their first comment, if variation in breaker clearing time exists so that use of two statistically meaningful extreme values (e.g., $\pm 4\sigma$ from the mean) lead to significant horizontal shifts in the maximum distance functions (see Figure 3 in the pa-

Authorized licensed use limited to: Wuhan University. Downloaded on February 10,2024 at 11:16:48 UTC from IEEE Xplore. Restrictions apply.

per), then probabilistic modeling of breaker clearing time should be considered. We have not considered this influence in our paper in order to introduce the essential concepts while maintaining standard industry practices where possible, which include using a fixed four cycle clearing time for EHV breakers when determining stability-related operating limits.

The discussers' second comment concerns our use of the homogeneous Poisson process to model occurrence of the event E_i, where we use in eqt. (7) $P(E_i) = \lambda_i e^{-\lambda_i}$, which provides the probability of having exactly one event in the next time period. The discussers correctly point out that our calculation excludes the probability of having more than one event occur in the time period. This is intentional and reflects the operator's concern for the *next* contingency and not the next $x > 1$ contingencies. To avoid the problem of nonnegligible probability for $x > 1$, risk calculations should be done for a much shorter time period, e.g., one hour or one day. In this case, the probability of occurrence of more than one event in the first time interval is negligible, and the probability of occurrence of more than zero events equals the probability of occurrence of one event, i.e.,

$$P_{x>0}(E_i) = 1 - e^{-\lambda_i} \approx 1 - (1 - \lambda_i) = \lambda_i$$
$$P_{x=1}(E_i) = \lambda_i e^{-\lambda_i} \approx \lambda_i$$

where the approximations improve as λ_i approaches zero, or equivalently, as we decrease the length of the unit time interval on which λ_i is based. For the events considered in the paper, choosing a one hour time interval for computation of risk causes λ_i to change to 3.47E-5, 11.8E-5, and 5.30E-5 events/hour for $i = 1, 2, 3$, respectively.

The discussers' third comment concerns the use of nonuniform outage rates. We agree that in order to use different Poisson intensities for different seasons and weather conditions, the time period should be shorter than one year. This conclusion is consistent with our response to the second comment.

The typographical error mentioned in the fourth comment occurs in Sections 3.4, 3.5, and 3.6 on occurrences of B_{21p}, B_{32p}, C_{21}, and C_{32}. These should be B_{12p}, B_{23p}, C_{12}, and C_{23} in order to remain consistent with the notation B_{jip} and C_{ji}. Also, the discussers are correct in pointing out that in Table 4, k should be replaced by j.

Manuscript received November 6, 1996.

Authorized licensed use limited to: Wuhan University. Downloaded on February 10,2024 at 11:16:48 UTC from IEEE Xplore. Restrictions apply.